A 3-D Magnetic Equivalent Circuit of an Axial-Flux MEMS Micromotor with Dimension Minimization Analysis

Xiaofeng Ding[1], Guanliang Liu[1], Hong Guo[1] and Hua Bai[2]

[1]BeiHang University, Beijing 100191 China, dingxiaofeng@buaa.edu.cn
[2] Kettering University, Flint, MI 48504,USA, hbai@kettering.edu

This paper presents an axial-flux microelectromechanical systems based (MEMS) micromotor with dual rotors and 10mm diameter. The characteristics of MEMS micromotor are analyzed and modeled using a 3-D magnetic equivalent circuit (MEC) taking the leakage flux and fringing effect into account. Such methodology yields more accurate prediction of the flux distribution inside the machine, back electromotive force waveform and the torque. Furthermore, an investigation of the leakage flux and fringing effect on dimension reduction of the MEMS micromotor is processed. The feasibility of the proposed method is validated by the 3-D finite element analysis (FEA). Finally, the method is applied to design and manufacture the micromotor.

***Index Terms*— mircoelectomechanical systems (MEMS) mircomotor, magnetic equivalent circuit (MEC), leakage flux, finite element analysis (FEA).**

I. Introduction

Microelectromechanical systems （MEMS）were evolved from the microelectronic technology, which results in that electromagnetic motors at MEMS scale have not yet been explored clearly especially when the motors are assembled with permanent magnets (PMs) [1]. Although the axial flux MEMS PM motors benefit from the high power density, the fringing effect and leakage flux impedes the motor dimension reduction, which is one of popular research areas of the MEMS micromotors.

In order to investigate the micromotor's static characteristics, such as flux distribution, back electromotive (EMF), and torque, the 3-D magnetic equivalent circuit (MEC) model is developed for the micromotor in this paper. Meanwhile, the leakage flux and fringing effect are considered in the model, which provides more accurate prediction. The leakage flux and fringing effect are analytically expressed in terms of the motor dimension and the magnetic material properties [2]. The proposed method is validated by the 3-D finite element analysis (FEA) and used to design a micromotor with the enhanced performance.

II. Axial-Flux MEMS Micromotors

Fig.1 shows the fundamental structure of an axial-flux MEMS micromotor. The stator coils are manufactured on a silicon chip with the deep etching processing. The ring-shaped PMs are assembled over the rotor yoke. Two rotors are symmetrically distributed on two sides of the stator, which increases the output torque, as well as avoids one-side asymmetric magnetic force [3], [4]. Furthermore, the stator without the iron core benefits from no iron loss. The surface mounted coils could increase the current density thanks for the cooling air induced by rotor running. The motor has three phases and 18 coils totally, as shown in Fig 1b, resulting in 6 coils in series connection (red, blue and yellow coils) per phase.

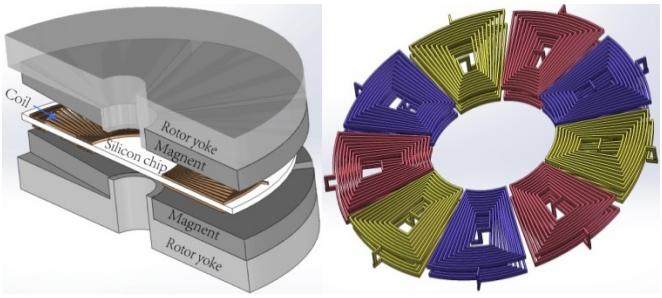

(a) (b)

Fig.1. The structure of an axial-flux MEMS micromotor.(a) total topology. (b) coils.

III. MEC Modeling

Fig. 2a shows the micromotor topology with the magnetic loop. Magnet-to-rotor and magnet-to-magnet leakage flux is pictured by blue and green lines, respectively with the main-loop flux in red. The fringing effect exists at the external and internal radius of the magnets, as shown in Fig.2b. The circular-arc straight-line permeance model is used for modeling the flux flow in the air gap [2], [5]. The reluctances of magnet to rotor R_{mr} and magnet to magnet R_{mm} are calculated taking the radial length of magnet in 3D space into account. The tangential length of magnets is considered when calculating fringing reluctances R_e and R_i . All the above reluctances can be expressed as Eqns. (1)-(4). Other reluctance expressions will be shown in the full paper. The equivalent magnet circuit is proposed in Fig.3.

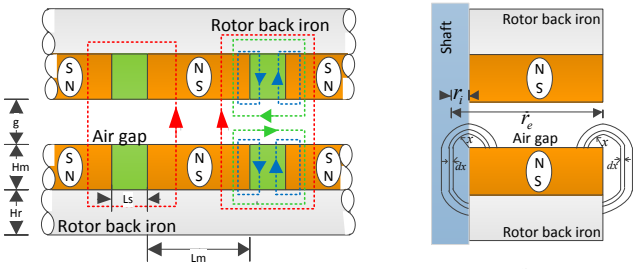

(a) (b)

Fig.2. Magnetic loop of the axial-flux micromotor. (a) Leakage fluxes. (b) Fringing effect.

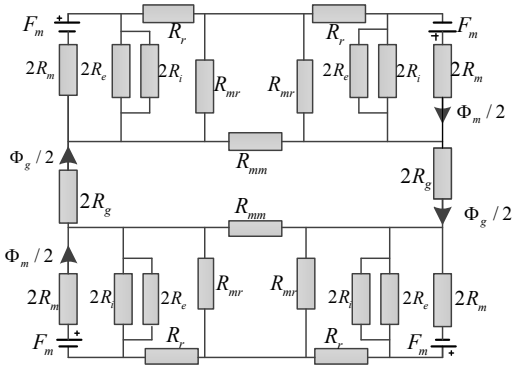

Fig.3. Equivalent magnetic lumped circuit for Fig.2

$$R_{mr}=1/[\frac{1}{L_e-L_i}(\int_{L_i}^{L_e}dL_s\int_0^{\frac{L_s}{2}}\frac{\mu_0 L}{H_m+\pi x}dx)]=1/\{\frac{1}{L_e-L_i}[\int_{L_i}^{L_e}\frac{\mu_0 L}{\pi}\ln(1+\frac{\pi\frac{L_s}{2}}{H_m})dL_s]\} \quad (1)$$

$$R_{mm}=1/[\frac{1}{L_e-L_i}(\int_{L_i}^{L_e}dL_s\int_0^{\frac{L_m}{2}}\frac{\mu_0 L}{L_s+\pi x}dx)]=1/\{\frac{1}{L_e-L_i}[\int_{L_i}^{L_e}\frac{\mu_0 L}{\pi}\ln(1+\frac{\pi\frac{g}{2}}{L_s})dL_s]\} \quad (2)$$

$$R_e=1/(\int_0^y\frac{\mu_0 L_{em}}{\frac{3}{2}\pi x+H_m}dx)=1/[\frac{\mu_0 L_{em}}{\frac{3}{2}\pi}\ln(1+\frac{\frac{3}{2}\pi y}{H_m})] \quad (3)$$

$$R_i=1/(\int_0^y\frac{\mu_0 L_{im}}{\frac{3}{2}\pi x+H_m}dx)=1/[\frac{\mu_0 L_{im}}{\frac{3}{2}\pi}\ln(1+\frac{\frac{3}{2}\pi y}{H_m})] \quad (4)$$

where $L_{em}=\theta\cdot r_e$, $L_{im}=\theta\cdot r_i$ and $L=r_e-r_i$, θ is the radian of one magnet, $L_e=(\pi/p-\theta)\cdot r_e$, $L_i=(\pi/p-\theta)\cdot r_i$, and p is the number of pole pairs. The variable y also depends on the motor dimension and the magnetic material properties.

IV. Results and Discussion

The average flux density in the air gap is shown in Fig.4. Due to the fringing effect and leakage flux occupying more percentage of the total flux when the diameter decreases, the air-gap flux interacting with the armature to produce the torque reduces significantly, described as the red line in Fig.4. Such outcome indicates the dimension minimization of the MEMS micromotor highly relies on effective reduction of the fringing effect and leakage flux. The blue line is the flux in the air gap without considering the fringing effect and leakage flux. The FEA results indicate that the proposed MEC could provide more accurate prediction. Fig.5 illustrated the machine with a 10mm diameter designed by the MEMS technology. The back EMF calculated by the proposed MEC is consist with the experimental results, as shown in Fig.6.

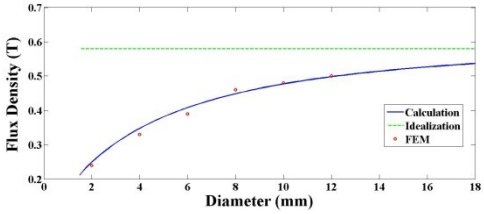

Fig.4. Flux density within air gap

TABLE I
Specification of The Micromotor

Parameter	Symbol	Value
Rated current (A)	i	0.1
Rated speed (rpm)	v	20000
Stator external diameter (mm)	r_e	10
Stator internal diameter (mm)	r_i	2.5
Magnet height (mm)	H_m	0.75
Magnet pole arc ratio	-	0.85
Rotor back iron height (mm)	H_r	1.5
Air-gap length (mm)	g	1.6
Pole pairs	p	3

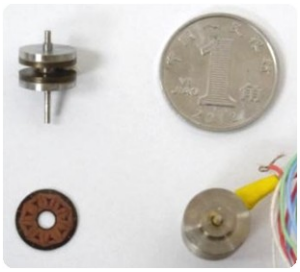

Fig.5. The real MEMS micromotor with 10mm diameter

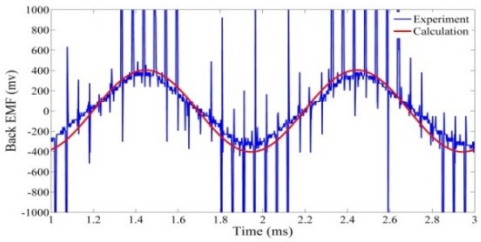

Fig.6. Back EMF from experiments and calculation

V. Conclusion

In this paper a 3-D MEC model of the axial-flux MEMS micromotor is developed. The model provided better accuracy of predicting the motor static characteristics due to taking the leakage fluxes and fringing effect into account. The proposed method is validated by the 3-D FEA, revealing that the fringing effect and leakage flux has the side effect on the dimension minimization of the machine. Finally, a suitable micromotor is designed and manufactured to verify the design methodology.

VI. References

[1] Merzaghi, S.; Koechli, C.; Perriard, Y., "Development of a Hybrid MEMS BLDC Micromotor," *Industry Applications, IEEE Transactions on* , vol.47, no.1, pp.3,11, Jan.-Feb. 2011

[2] Ronghai Qu; Lipo, T.A., "Analysis and modeling of air-gap and zigzag leakage fluxes in a surface-mounted permanent-magnet Machine," *Industry Applications, IEEE Transactions on* , vol.40, no.1, pp.121,127, Jan.-Feb. 2004

[3] Yunkai Huang; Baoyun Ge; Jianning Dong; Heyun Lin; Jianguo Zhu; Youguang Guo, "3-D Analytical Modeling of No-Load Magnetic Field of Ironless Axial Flux Permanent Magnet Machine," *Magnetics, IEEE Transactions on* , vol.48, no.11, pp.2929,2932, Nov. 2012

[4] Mahmoudi, A.; Kahourzade, S.; Rahim, N.A.; Hew, W.P., "Design, Analysis, and Prototyping of an Axial-Flux Permanent Magnet Motor Based on Genetic Algorithm and Finite-Element Analysis," *Magnetics, IEEE Transactions on* , vol.49, no.4, pp.1479,1492, April 2013

[5] Yunkai Huang; Tao Zhou; Jianning Dong; Heyun Lin; Hui Yang; Ming Cheng, "Magnetic Equivalent Circuit Modeling of Yokeless Axial Flux Permanent Magnet Machine With Segmented Armature," *Magnetics, IEEE Transactions on* , vol.50, no.11, pp.1,4, Nov. 2014